

# Usefulness of $^{11}\text{C}$ -Methionine for Differentiating Tumors from Granulomas in Experimental Rat Models: A Comparison with $^{18}\text{F}$ -FDG and $^{18}\text{F}$ -FLT

Songji Zhao<sup>1</sup>, Yuji Kuge<sup>2,3</sup>, Masashi Kohanawa<sup>4</sup>, Toshiyuki Takahashi<sup>5</sup>, Yan Zhao<sup>1</sup>, Min Yi<sup>4</sup>, Kakuko Kanegae<sup>1</sup>, Koh-ichi Seki<sup>6</sup>, and Nagara Tamaki<sup>1</sup>

<sup>1</sup>Department of Nuclear Medicine, Graduate School of Medicine, Hokkaido University, Sapporo, Japan; <sup>2</sup>Department of Molecular Imaging, Graduate School of Medicine, Hokkaido University, Sapporo, Japan; <sup>3</sup>Department of Patho-Functional Bioanalysis, Graduate School of Pharmaceutical Sciences, Kyoto University, Kyoto, Japan; <sup>4</sup>Department of Microbiology, Graduate School of Medicine, Hokkaido University, Sapporo, Japan; <sup>5</sup>Department of Pathology, Hokkaido Gastroenterology Hospital, Sapporo, Japan; and <sup>6</sup>Central Institute of Isotope Science, Hokkaido University, Sapporo, Japan

Many clinical PET studies have shown that increased  $^{18}\text{F}$ -FDG uptake is not specific to malignant tumors.  $^{18}\text{F}$ -FDG is also taken up in inflammatory lesions, particularly in granulomatous lesions such as sarcoidosis or active inflammatory processes after chemoradiotherapy, making it difficult to differentiate malignant tumors from benign lesions, and is the main source of false-positive  $^{18}\text{F}$ -FDG PET findings in oncology. These problems may be overcome by multitracer studies using 3'-deoxy-3'- $^{18}\text{F}$ -fluorothymidine ( $^{18}\text{F}$ -FLT) or L- $^{11}\text{C}$ -methionine. However,  $^{18}\text{F}$ -FLT or  $^{11}\text{C}$ -methionine uptake in granulomatous lesions remains unclarified. In this study, the potentials of  $^{18}\text{F}$ -FLT and  $^{11}\text{C}$ -methionine in differentiating malignant tumors from granulomas were compared with  $^{18}\text{F}$ -FDG using experimental rat models.

**Methods:** Dual-tracer tissue distribution studies using  $^{18}\text{F}$ -FDG and  $^3\text{H}$ -FLT (groups I and III) or  $^{18}\text{F}$ -FDG and  $^{14}\text{C}$ -methionine (groups II and IV) were performed on rats bearing both granulomas (*Mycobacterium bovis* bacillus Calmette-Guérin [BCG]-induced) and hepatomas (KDH-8-induced) (groups I and II) or on rats bearing both turpentine oil-induced inflammation and hepatomas (groups III and IV). One hour after the injection of a mixture of  $^{18}\text{F}$ -FDG and  $^3\text{H}$ -FLT or of  $^{18}\text{F}$ -FDG and  $^{14}\text{C}$ -methionine, tissues were excised to determine the radioactivities of  $^{18}\text{F}$ -FDG,  $^3\text{H}$ -FLT, and  $^{14}\text{C}$ -methionine (differential uptake ratio). **Results:** Mature epithelioid cell granuloma formation and massive lymphocyte infiltration were observed in the granuloma tissue induced by BCG, histologically similar to sarcoidosis. The granulomas showed high  $^{18}\text{F}$ -FDG uptake comparable to that in the hepatomas (group I,  $8.18 \pm 2.40$  vs.  $9.13 \pm 1.52$ ,  $P = \text{NS}$ ; group II,  $8.43 \pm 1.45$  vs.  $8.91 \pm 2.32$ ,  $P = \text{NS}$ ).  $^{14}\text{C}$ -Methionine uptake in the granuloma was significantly lower than that in the hepatoma ( $1.31 \pm 0.22$  vs.  $2.47 \pm 0.60$ ,  $P < 0.01$ ), whereas  $^3\text{H}$ -FLT uptake in the granuloma was comparable to that in the hepatoma ( $1.98 \pm 0.70$  vs.  $2.30 \pm 0.67$ ,  $P = \text{NS}$ ). Mean uptake of  $^{18}\text{F}$ -FDG,  $^3\text{H}$ -FLT, and  $^{14}\text{C}$ -methionine was markedly lower in the turpentine oil-induced inflammation than in the tumor. **Conclusion:**

$^{14}\text{C}$ -Methionine uptake was significantly lower in the granuloma than in the tumor, whereas  $^{18}\text{F}$ -FDG and  $^3\text{H}$ -FLT were not able to differentiate granulomas from tumors. These results suggest that  $^{14}\text{C}$ -methionine has the potential to accurately differentiate malignant tumors from benign lesions, particularly granulomatous lesions, providing a biologic basis for clinical PET studies.

**Key Words:**  $^{11}\text{C}$ -methionine; granuloma; inflammation; tumor; rat

**J Nucl Med 2008; 49:135–141**

DOI: 10.2967/jnumed.107.044578

As a useful tracer for tumor imaging with PET,  $^{18}\text{F}$ -FDG has been widely applied to tumor detection, staging, evaluation of treatment response, and differentiation of malignant tumors from benign lesions in clinical oncology (1,2). These applications are based on the increased  $^{18}\text{F}$ -FDG uptake due to enhanced glucose use in most tumors. Recent investigations, including many clinical PET studies, however, have shown that increased  $^{18}\text{F}$ -FDG uptake is not specific to malignant tumors (3–7).  $^{18}\text{F}$ -FDG is also taken up in inflammatory lesions, particularly in granulomatous lesions such as sarcoidosis or active inflammatory processes after chemoradiotherapy (3–7), making it difficult to differentiate malignant tumors from benign lesions, and is the main source of false-positive  $^{18}\text{F}$ -FDG PET findings in oncology (8). It has been suggested that these problems may be overcome by multitracer studies using 3'-deoxy-3'- $^{18}\text{F}$ -fluorothymidine ( $^{18}\text{F}$ -FLT) or L- $^{11}\text{C}$ -methionine (8,9).

$^{18}\text{F}$ -FLT, a radiolabeled analog of thymidine, has been developed as a PET tracer to image cellular proliferation in vivo (10).  $^{18}\text{F}$ -FLT is phosphorylated by the enzyme thymidine kinase 1, which leads to intracellular trapping of the tracer. During DNA synthesis, thymidine kinase 1 activity increases almost 10-fold and is thus an accurate reflection of cellular proliferation (8,11). On the other hand,  $^{11}\text{C}$ -methionine

Received Jun. 25, 2007; revision accepted Sep. 18, 2007.

For correspondence or reprints contact: Nagara Tamaki, MD, PhD, Department of Nuclear Medicine, Graduate School of Medicine, Hokkaido University, Kita 15 Nishi 7, Kita-ku, Sapporo 060-8638, Japan.

E-mail: natamaki@med.hokudai.ac.jp

COPYRIGHT © 2008 by the Society of Nuclear Medicine, Inc.

uptake reflects increased amino acid transport and protein synthesis and is related to cellular proliferation.  $^{11}\text{C}$ -Methionine has been shown to possess a high specificity in tumor detection, tumor delineation, and differentiation of benign from malignant lesions (12,13) because of the lower uptake of  $^{11}\text{C}$ -methionine than of  $^{18}\text{F}$ -FDG in inflammatory cells (14–16). These factors suggest that thymidine or amino acid tracers are potentially more suitable than  $^{18}\text{F}$ -FDG for the differentiation of tumors from inflammatory lesions. However, the uptake of these tracers in granulomatous lesions remains unclarified, mainly because of the lack of suitable animal models. In this regard, we have recently developed a rat model of intramuscular granuloma characterized by epithelioid cell granuloma formation and massive lymphocyte infiltration around the granuloma, histologically similar to sarcoidosis (17). The rat granuloma showed high  $^{18}\text{F}$ -FDG uptake comparable to that in the tumor, indicating the usefulness of our model for studies of differential diagnosis.

The purpose of this study was to compare the potentials of  $^{18}\text{F}$ -FLT and  $^{11}\text{C}$ -methionine with  $^{18}\text{F}$ -FDG for differentiating malignant tumors from granulomas in the rat model bearing granuloma and tumor.

## MATERIALS AND METHODS

### Radiopharmaceuticals

$^{18}\text{F}$ -FDG, synthesized by standard procedures, was obtained from Hokkaido University Hospital Cyclotron Facility. L-[methyl- $^{14}\text{C}$ ]methionine (specific activity, 1.48–2.04 GBq/mmol) and [methyl- $^3\text{H}$  (N)]-3'-fluoro 3'-deoxythymidine ( $^3\text{H}$ -FLT) (specific activity, 74–370 GBq/mmol) were purchased from American Radiolabeled Chemicals, Inc., and Moravек Biochemicals Inc.

### Animal Studies

All experimental protocols were approved by the Laboratory Animal Care and Use Committee of Hokkaido University. Eight-week-old male Wistar King Aptekman/hok rats (supplied by Japan SLC, Inc.) were used in all experiments. The *Mycobacterium bovis* bacillus Calmette-Guérin (BCG), a Japanese strain, was grown on

Middlebrook 7H11 agar (Difco Laboratories), suspended in phosphate-buffered saline with 0.05% polysorbate 20, and stocked at  $-80^\circ\text{C}$ . BCG ( $1 \times 10^7$  CFU/rat) and allogenic hepatoma cells (KDH-8,  $1 \times 10^6$  cells/rat) were inoculated, respectively, into the left and right calf muscles to generate a rat model bearing both the granuloma and the tumor. Turpentine oil (0.2 mL/rat) and KDH-8 were inoculated, respectively, into the left and right calf muscles to generate a rat model bearing both turpentine oil-induced inflammation and tumor. Figure 1 shows the experimental protocols of the animal studies. At designated periods after inoculation of KDH-8 and BCG or of KDH-8 and turpentine, the rats were kept fasting overnight, anesthetized with pentobarbital (50 mg/kg of body weight, intraperitoneally), and administered an intravenous injection of a mixture of  $^{18}\text{F}$ -FDG (7.4 MBq) and  $^3\text{H}$ -FLT (0.185 MBq) or of  $^{18}\text{F}$ -FDG (7.4 MBq) and  $^{14}\text{C}$ -methionine (0.185 MBq). The rats were kept under anesthesia throughout the experiment. To decrease the serum level of endogenous thymidine, the rats were pretreated with thymidine phosphorylase (1,000 U/kg of body weight) 45 min before the injection of a mixture of  $^{18}\text{F}$ -FDG and  $^3\text{H}$ -FLT, according to the procedures reported by van Waarde et al. (8). Sixty minutes after the injection of a mixture of  $^{18}\text{F}$ -FDG and  $^3\text{H}$ -FLT or of  $^{18}\text{F}$ -FDG and  $^{14}\text{C}$ -methionine, the animals were sacrificed, and tumor, granuloma, inflammatory tissues, and other organs were excised. The tissues and blood samples were weighed, and  $^{18}\text{F}$ -FDG radioactivity was determined using a  $\gamma$ -counter (1480 WIZARD 3"; Wallac Co., Ltd.). The samples were then solubilized with Soluene 350 (Packard Bioscience B.V.), and  $^3\text{H}$ -FLT or  $^{14}\text{C}$ -methionine radioactivity was measured using a liquid scintillation counter (LSC-5100; Aloka Co., Ltd.).  $^{18}\text{F}$ -FDG,  $^3\text{H}$ -FLT, and  $^{14}\text{C}$ -methionine uptake levels in the tissues were expressed as a differential uptake ratio (DUR) (cpm measured per gram of tissue/cpm injected per gram of body weight) (16). The lesion (tumor, granuloma, or turpentine-induced inflammatory tissue)-to-muscle (L/M) ratios and the lesion-to-blood (L/B) ratios of  $^{18}\text{F}$ -FDG,  $^3\text{H}$ -FLT, and  $^{14}\text{C}$ -methionine uptake were calculated from the DUR value of each tissue (18,19). Samples from the tumor, granuloma, and turpentine oil-induced inflammatory tissues were formalin-fixed and paraffin-embedded for the subsequent histologic staining. Blood samples for glucose level measurement were obtained immediately before the tracer injection and immediately before sacrifice. Blood glucose

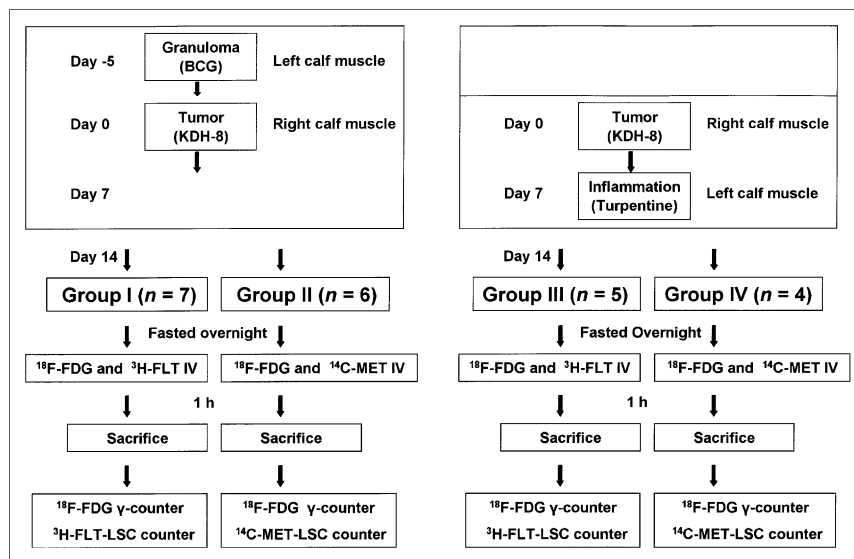


**FIGURE 1.** Experimental protocols of this study. LSC = liquid scintillation counter.

level was determined using a biochemical analyzer (MediSense; Dainobot Co., Ltd.).

### Histochemical Studies

Formalin-fixed, paraffin-embedded 3- $\mu$ m-thick sections of tumor, granuloma, and turpentine oil-induced inflammation tissue were stained with hematoxylin and eosin. The immunohistochemical staining of an immune-associated antigen (Ia) was also performed using a monoclonal antibody (mAb) (mouse IgG, MRC OX-6; Oxford Biotechnology Ltd.) that recognizes a monomorphic determinant of rat Ia, MHC class II, present on B lymphocytes, dendritic cells, some macrophages, and certain epithelial cells, as previously described (17).

### Statistical Analysis

All values are expressed as mean  $\pm$  SD. The nonparametric Kruskal–Wallis test was used to assess the significance of differences in blood glucose levels among the 4 groups of rats. Statistical analyses were performed using a nonparametric Mann–Whitney *U* test to evaluate the significance of differences in values between the 2 types of lesions (tumor vs. granuloma or tumor vs. turpentine-induced inflammation). A value of *P* less than 0.05 was considered significant.

## RESULTS

### Blood Glucose Level and Histopathologic Findings

There was no statistically significant difference in blood glucose levels among the 4 groups of rats at the times of injection and sacrifice (Table 1). The blood glucose levels were within the physiologic range.

In the intramuscular granuloma induced by BCG, the granulomatous lesions showed mature epithelioid cell granuloma formation and massive lymphocyte infiltration around the granuloma (Fig. 2A). Immunohistochemical staining also showed the accumulation of Ia-positive macrophages and Ia-positive lymphocytes in the periphery of the granuloma (Fig. 2B). In the intramuscular tumor induced by KDH-8 cells, massive viable and proliferating cancer cells were observed by hematoxylin-and-eosin staining (Fig. 2C). In the turpentine-induced inflammatory tissue, massive neutrophil infiltration and ambient connective tissue formation were observed around the site of turpentine oil injection (Fig. 2D).

### Uptake of $^{18}\text{F}$ -FDG, $^3\text{H}$ -FLT, and $^{14}\text{C}$ -Methionine

$^{18}\text{F}$ -FDG,  $^3\text{H}$ -FLT, and  $^{14}\text{C}$ -methionine uptake in the tumor, granuloma, and turpentine-induced inflammatory tissues are summarized in Figure 3 and Table 2.

Figures 3A and 3B show the tracer uptake levels in rats bearing the tumor and granuloma (groups I and II). The granuloma showed high  $^{18}\text{F}$ -FDG uptake comparable to that in the tumor (group I,  $8.18 \pm 2.40$  DUR for granuloma vs.  $9.13 \pm 1.52$  DUR for tumor, *P* = NS; group II,  $8.43 \pm 1.45$  DUR for granuloma vs.  $8.91 \pm 2.32$  DUR for tumor, *P* = NS).  $^3\text{H}$ -FLT uptake in the granuloma was also comparable to that in the tumor (group I,  $1.98 \pm 0.70$  DUR for granuloma vs.  $2.30 \pm 0.67$  DUR for tumor, *P* = NS). Mean  $^{14}\text{C}$ -methionine uptake in the granuloma was significantly lower than that in the tumor (group II,  $1.31 \pm 0.22$  DUR for granuloma vs.  $2.47 \pm 0.60$  DUR for tumor, *P* < 0.01).  $^{14}\text{C}$ -Methionine uptake in the granuloma was about 53% of that in the tumor (Fig. 3B).

In rats bearing the tumor and turpentine oil-induced inflammatory tissue (Figs. 3C and 3D, groups III and IV), the mean  $^{18}\text{F}$ -FDG uptake in the inflammatory tissue was markedly lower than that in the tumor (group III,  $2.42 \pm 0.43$  DUR for inflammatory tissue vs.  $9.13 \pm 0.50$  DUR for tumor, *P* < 0.01; group IV,  $3.99 \pm 0.22$  DUR for inflammatory tissue vs.  $11.14 \pm 1.03$  DUR for tumor, *P* < 0.05).  $^3\text{H}$ -FLT and  $^{14}\text{C}$ -methionine uptake was also significantly lower in the inflammatory tissue than in the tumor (group III,  $^3\text{H}$ -FLT,  $0.99 \pm 0.13$  DUR for inflammatory tissue vs.  $2.66 \pm 0.13$  DUR for tumor, *P* < 0.01; group IV,  $^{14}\text{C}$ -methionine,  $1.77 \pm 0.18$  for inflammatory tissue vs.  $2.96 \pm 0.57$  DUR for tumor, *P* < 0.05).

The L/M and the L/B ratios of  $^{18}\text{F}$ -FDG,  $^3\text{H}$ -FLT, and  $^{14}\text{C}$ -methionine uptake are summarized in Table 2. The mean L/M and L/B ratios of  $^{18}\text{F}$ -FDG and  $^3\text{H}$ -FLT uptake in the granuloma were comparable to those in the tumor (group I, *P* = NS). However, the mean L/M and L/B ratios of  $^{14}\text{C}$ -methionine uptake in the granuloma was significantly lower than those in the hepatoma (group II,  $3.0 \pm 0.6$  vs.  $5.7 \pm 1.9$  for L/M and  $1.8 \pm 0.3$  vs.  $3.5 \pm 1.0$  for L/B, *P* < 0.01, respectively). The L/M and L/B ratios of  $^{18}\text{F}$ -FDG,  $^3\text{H}$ -FLT, and  $^{14}\text{C}$ -methionine uptake in the turpentine-induced inflammation were markedly lower than those in the tumor (groups III and IV).

## DISCUSSION

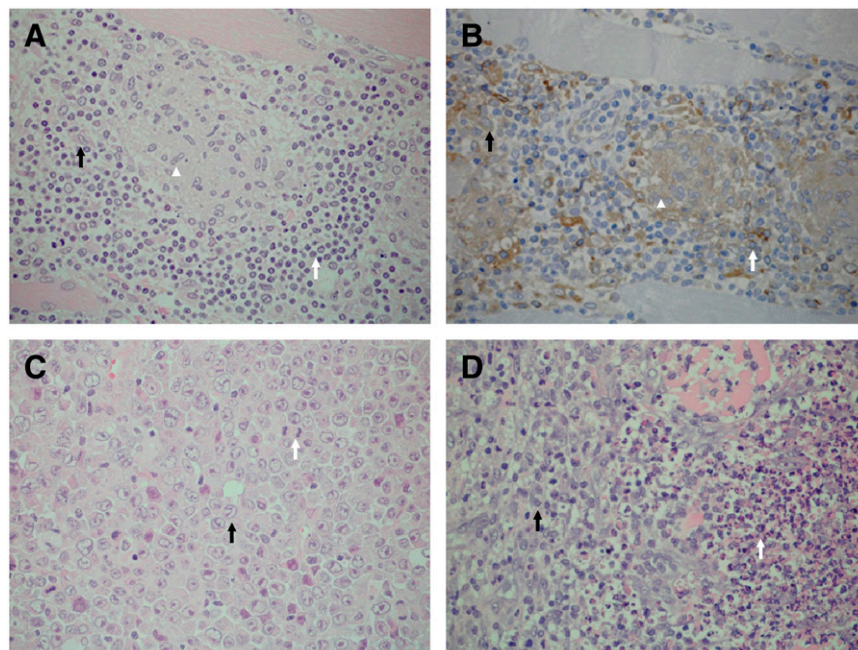
This study showed that  $^{14}\text{C}$ -methionine uptake in the granuloma was about 50% of that in the tumor (Fig. 3B), and the difference was significant. In contrast,  $^{18}\text{F}$ -FLT and  $^{18}\text{F}$ -FDG uptake in the granuloma was comparable to that in

**TABLE 1**  
Blood Glucose Levels (mg/dL)

Time	Group I ( <i>n</i> = 7): $^{18}\text{F}$ -FDG + $^3\text{H}$ -FLT	Group II ( <i>n</i> = 6): $^{18}\text{F}$ -FDG + $^{14}\text{C}$ -methionine	Group III ( <i>n</i> = 5): $^{18}\text{F}$ -FDG + $^3\text{H}$ -FLT	Group IV ( <i>n</i> = 4): $^{18}\text{F}$ -FDG + $^{14}\text{C}$ -methionine
At tracer injection	$87.7 \pm 7.4$	$93.2 \pm 6.5$	$84.2 \pm 8.5$	$87.3 \pm 5.2$
At sacrifice	$88.0 \pm 6.7$	$86.0 \pm 5.7$	$91.0 \pm 8.0$	$85.3 \pm 2.2$

Data are mean  $\pm$  SD.

**FIGURE 2.** Microscopy images ( $\times 400$ ) of hematoxylin-and-eosin staining (granuloma [A], tumor [C], and turpentine-induced inflammation [D]) and immunostaining for Ia antigen (granuloma [B]). (A) Intramuscular granuloma induced by BCG shows mature epithelioid cell granuloma formation and massive lymphocyte infiltration around granuloma. (B) Immunostaining for Ia antigen shows infiltrations of Ia-positive epithelioid cells and macrophages in granuloma and Ia-positive lymphocytes in periphery of granuloma. In A and B, arrowhead indicates epithelioid cell granuloma; white arrow, lymphocyte infiltration; and black arrow, macrophage infiltration. (C) Massive viable and proliferating cancer cells in tumor tissue. Black arrow indicates viable cancer cell; white arrow, proliferating cancer cell (mitotic division). (D) Massive neutrophil infiltration and ambient connective tissue formation were observed around site of turpentine oil injection. White arrow indicates neutrophil infiltration; black arrow, connective tissue.



the tumor. These results suggest the possible usefulness of  $^{11}\text{C}$ -methionine for differentiating malignant tumors from benign lesions, providing a biologic basis for clinical PET studies.

The present results suggest that amino acid tracers are potentially more suitable than  $^{18}\text{F}$ -FDG for the differentiation of tumors from inflammation, including granuloma. Our results are consistent with previous clinical findings that showed that  $^{18}\text{F}$ -FDG uptake is significantly higher than  $^{11}\text{C}$ -methionine uptake in mediastinal bilateral hilar lymphadenopathy with sarcoidosis (20). On the other hand, to the best of our knowledge, this is the first report on radiolabeled  $^{14}\text{C}$ -methionine uptake in an experimental granuloma, although studies of  $^{14}\text{C}$ -methionine uptake in inflammation induced by intramuscular injections of croton oil and carrageenan (21) have been reported.

It is of great importance to determine the cause of the difference between  $^{11}\text{C}$ -methionine and  $^{18}\text{F}$ -FDG accumulations in granulomas. Cellular uptake of  $^{18}\text{F}$ -FDG in sarcoidosis is considered to be related to inflammatory cell infiltrates, which are composed of lymphocytes, macrophages, and epithelioid cells from monocytes, because  $^{18}\text{F}$ -FDG has been observed in vitro to be accumulated by leukocytes (22,23), lymphocytes, and macrophages (24). An increased  $^{18}\text{F}$ -FDG distribution level was observed mainly in epithelioid cell granulomas by autoradiography, whereas the  $^{14}\text{C}$ -methionine distribution level was low. The activities of granuloma formation and granuloma-associated immune cells may be reflected by the accumulation of  $^{18}\text{F}$ -FDG but not by that of  $^{14}\text{C}$ -methionine, although the detailed mechanisms underlying the accumulation of these tracers in granulomas remain unclarified. As for the accumulation of these tracers in tumors, Kubota et al. (15)

have demonstrated by a microautoradiographic study that  $^{14}\text{C}$ -methionine uptake is achieved largely by viable cancer cells, whereas uptake by macrophages and granulation tissues is low, in contrast to  $^{18}\text{F}$ -FDG. An increased  $^{18}\text{F}$ -FDG accumulation in young granulation tissues around a tumor and in macrophages infiltrating the margins of an extensive area of tumor necrosis was observed by microautoradiography using  $^{18}\text{F}$ -FDG and  $^3\text{H}$ -deoxyglucose (24). The distinctive uptake profiles of  $^{18}\text{F}$ -FDG and  $^{11}\text{C}$ -methionine may provide information on the different roles of these tracers in the diagnosis of tumors and inflammation.

This study showed that mean  $^3\text{H}$ -FLT uptake in the BCG-induced granuloma was comparable to that in the KDH-8-induced hepatoma, as in the case of  $^{18}\text{F}$ -FDG, although the level of  $^3\text{H}$ -FLT uptake was lower than that of  $^{18}\text{F}$ -FDG. Some investigators reported that  $^{18}\text{F}$ -FLT uptake in inflammatory cells is lower than that in tumors, because the mitotic activity of inflammatory cells is lower than that of tumor cells. Van Waarde et al. reported that  $^{18}\text{F}$ -FLT uptake in turpentine-induced inflammation is 32% of that in C6 rat gliomas (8), suggesting a high tumor specificity of  $^{18}\text{F}$ -FLT (8). Our results for turpentine-induced inflammatory tissue were consistent with previous reports. In contrast,  $^3\text{H}$ -FLT uptake in the granuloma was comparable to that in the hepatoma. Clinical studies (25) also showed that a patient with granulomas after radiation and chemotherapy showed increased  $^{18}\text{F}$ -FLT uptake. A patient with nonspecific interstitial pneumonia had a false-positive  $^{18}\text{F}$ -FLT finding (Ki-67 index, 15%) (26). Inflammatory lung diseases are accompanied by lymphocyte infiltration and involve growth factors that enhance the proliferation of lymphocytes (27). These findings suggest that  $^{18}\text{F}$ -FLT may accumulate in chronic granulomatous lesions with proliferative inflammation. Our

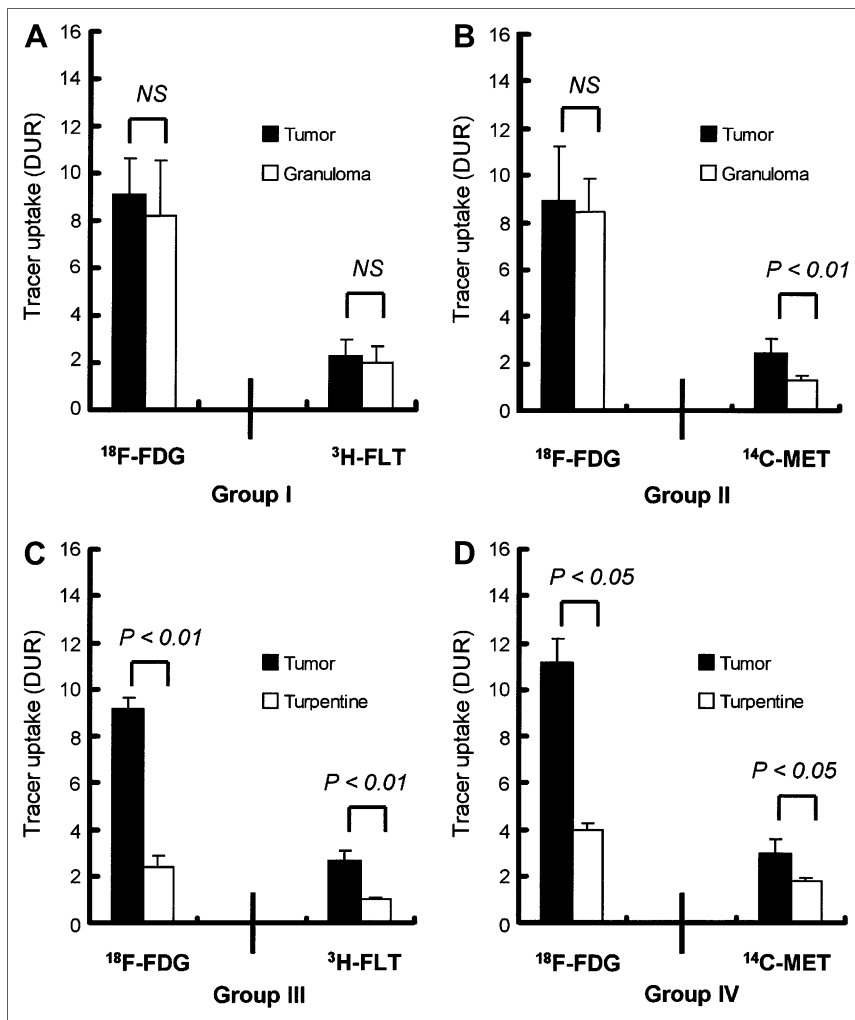


**FIGURE 3.** <sup>18</sup>F-FDG, <sup>3</sup>H-FLT, and <sup>14</sup>C-methionine uptake in tumor, granuloma, and turpentine oil-induced inflammation. (A) Group I: <sup>18</sup>F-FDG and <sup>3</sup>H-FLT uptake in tumor and granuloma. (B) Group II: <sup>18</sup>F-FDG and <sup>14</sup>C-methionine uptake in tumor and granuloma. (C) Group III: <sup>18</sup>F-FDG and <sup>3</sup>H-FLT uptake in tumor and turpentine oil-induced inflammation. (D) Group IV: <sup>18</sup>F-FDG and <sup>14</sup>C-methionine uptake in turpentine oil-induced inflammation. Values are mean  $\pm$  SD. NS = not statistically significant.

study showed the accumulation of Ia-positive lymphocytes in the periphery of the granuloma (Fig. 2B) (Ki-67 index, 6.3%), possibly explaining the increased <sup>3</sup>H-FLT uptake in the granulomatous lesions. Thus, our experimental results support previous clinical findings, although detailed investigations, including that of the correlation between the Ki-67 proliferation index and <sup>18</sup>F-FLT distribution in the granuloma and tumor using autoradiography, are required.

Although the usefulness of <sup>11</sup>C-methionine for differentiating malignant tumors from benign lesions was indicated in our experimental models, uptake of <sup>18</sup>F-FLT and <sup>11</sup>C-methionine by tumor was relatively lower than uptake of <sup>18</sup>F-FDG. An absolute uptake level is also a determinant of the usefulness of radiopharmaceuticals. General tumor detectability might be higher with <sup>18</sup>F-FDG than with others, although several clinical and experimental studies suggested that <sup>18</sup>F-FDG and <sup>11</sup>C-methionine were equally useful in detecting residual or recurrent malignant tumors (16,28).

It is important to note the limitations of our study. We measured the biodistribution of <sup>14</sup>C-methionine at 60 min after injection, to avoid technical complications. In clinical settings, however, PET images of <sup>11</sup>C-methionine are usually

acquired at 10–30 min after injection, because of the short half-life of <sup>11</sup>C. To investigate whether the biodistribution of <sup>14</sup>C-methionine at early time points provides data similar to those of the present study (at 60 min) in differentiating the tumor from the granuloma, we preliminarily performed biodistribution studies at 5, 15, and 30 min after the <sup>14</sup>C-methionine injection using the tumor and inflammation models. The findings showed that uptake of <sup>14</sup>C-methionine in the tumor and granuloma plateaued at 15–30 min after the injection. <sup>14</sup>C-Methionine uptake in the granuloma at 15 and 30 min was also significantly lower than that in the tumor—61% and 45%, respectively, of tumor uptake. These results were consistent with the present results, although <sup>14</sup>C-methionine uptake in the tumor and granuloma at 60 min was lower than that at 15 and 30 min. The biodistribution at early time points supports our results in the present study. It should also be noted that uptake of <sup>14</sup>C-methionine in normal organs was relatively high in our rats. This result may be ascribed to the time point (60 min after injection) at which we performed the <sup>14</sup>C-methionine biodistribution study. Kubota et al. (29) reported that the distribution of <sup>14</sup>C-methionine in abdominal organs including the liver, intestine, and kidney

**TABLE 2**  
Uptake Levels, L/M, and L/B 60 Minutes After Injection of <sup>18</sup>F-FDG, <sup>3</sup>H-FLT, and <sup>14</sup>C-Methionine (DUR)

Parameter	KDH-8 and BCG				KDH-8 and turpentine oil			
	Group I (n = 7)		Group II (n = 6)		Group III (n = 5)		Group IV (n = 4)	
	<sup>18</sup> F-FDG	<sup>3</sup> H-FLT	<sup>18</sup> F-FDG	<sup>14</sup> C-Methionine	<sup>18</sup> F-FDG	<sup>3</sup> H-FLT	<sup>18</sup> F-FDG	<sup>14</sup> C-Methionine
Blood	0.69 ± 0.14	0.91 ± 0.15	0.60 ± 0.11	0.71 ± 0.04	0.57 ± 0.08	0.72 ± 0.11	0.77 ± 0.10	0.99 ± 0.03
Plasma	0.95 ± 0.25	0.85 ± 0.12	0.59 ± 0.13	0.95 ± 0.04	0.66 ± 0.11	0.74 ± 0.08	0.79 ± 0.10	1.37 ± 0.08
Muscle	0.28 ± 0.05	0.85 ± 0.09	0.31 ± 0.11	0.45 ± 0.06	0.20 ± 0.03	0.74 ± 0.07	0.30 ± 0.03	0.41 ± 0.04
Brown fat	0.52 ± 0.48	0.48 ± 0.25	0.33 ± 0.06	0.42 ± 0.07	0.38 ± 0.08	0.43 ± 0.05	0.44 ± 0.03	0.50 ± 0.03
White fat	0.18 ± 0.03	0.16 ± 0.05	0.18 ± 0.02	0.11 ± 0.02	0.21 ± 0.08	0.22 ± 0.09	0.19 ± 0.02	0.13 ± 0.01
Heart	1.04 ± 0.60	0.86 ± 0.10	0.62 ± 0.27	0.83 ± 0.05	0.54 ± 0.05	0.72 ± 0.09	0.60 ± 0.13	0.97 ± 0.03
Brain	3.05 ± 0.24	0.15 ± 0.02	2.97 ± 0.15	0.48 ± 0.03	2.69 ± 0.16	0.16 ± 0.07	3.49 ± 0.46	0.64 ± 0.04
Lung	2.35 ± 0.70	1.51 ± 0.27	1.16 ± 0.13	1.30 ± 0.03	2.51 ± 0.33	1.72 ± 0.25	1.52 ± 0.08	1.63 ± 0.06
Thymus	1.89 ± 0.33	1.03 ± 0.39	2.16 ± 0.23	1.57 ± 0.11	1.20 ± 0.24	0.84 ± 0.46	2.46 ± 0.20	1.85 ± 0.30
Spleen	3.26 ± 0.82	4.20 ± 0.73	2.34 ± 0.26	2.16 ± 0.41	2.75 ± 0.30	5.06 ± 1.09	3.19 ± 0.20	3.03 ± 0.14
Liver	2.37 ± 0.64	1.71 ± 0.34	0.89 ± 0.22	7.15 ± 0.75	2.10 ± 0.40	1.42 ± 0.09	1.24 ± 0.11	7.97 ± 0.83
Kidney	2.06 ± 0.92	2.37 ± 0.38	1.31 ± 0.30	3.76 ± 0.14	1.36 ± 0.24	1.92 ± 0.15	2.98 ± 1.31	3.97 ± 0.23
Bone marrow	2.50 ± 0.35	9.42 ± 0.99	2.37 ± 0.24	3.33 ± 0.24	2.07 ± 0.36	11.93 ± 2.18	2.92 ± 0.14	4.69 ± 0.26
Tumor	9.13 ± 1.52	2.30 ± 0.67	8.91 ± 2.32	2.47 ± 0.60	9.13 ± 0.50	2.66 ± 0.41	11.14 ± 1.03	2.96 ± 0.57
Granuloma or turpentine	8.18 ± 2.40	1.98 ± 0.70	8.43 ± 1.45	1.31 ± 0.22*	2.42 ± 0.43*	0.99 ± 0.13*	3.99 ± 0.22*	1.77 ± 0.18†
Ratio								
L (tumor)/M	34.2 ± 9.8	2.7 ± 0.7	33.0 ± 16.8	5.7 ± 1.9	45.3 ± 6.5	3.6 ± 0.5	37.6 ± 1.5	7.2 ± 1.6
L (granuloma)/M or L (turpentine)/M	30.0 ± 9.3	2.3 ± 0.8	29.7 ± 9.6	3.0 ± 0.6*	11.9 ± 2.4*	1.3 ± 0.2*	13.6 ± 1.9†	4.3 ± 0.8†
L (tumor)/B	13.9 ± 4.4	2.6 ± 0.8	14.9 ± 2.7	3.5 ± 1.0	16.2 ± 1.7	3.8 ± 0.9	14.6 ± 1.7	3.0 ± 0.6
L (granuloma)/B or L (turpentine)/B	12.4 ± 5.1	2.2 ± 0.5	14.3 ± 2.5	1.8 ± 0.3*	4.3 ± 0.9*	1.4 ± 0.2*	5.3 ± 0.9*	1.8 ± 0.1†

\*P < 0.01, tumor vs. granuloma or tumor vs. turpentine-induced inflammation.  
†P < 0.05.

was still increased after 30 min after injection. Another limitation of our study was that only 1 tumor model was used to compare accumulation of the PET pharmaceuticals. Other tumor models should be used to confirm our preliminary results.

## CONCLUSION

Our experimental studies demonstrated that <sup>14</sup>C-methionine uptake in the granuloma was significantly lower than that in the tumor, whereas <sup>18</sup>F-FDG and <sup>3</sup>H-FLT were not able to differentiate the granuloma from the tumor. These results suggest that <sup>14</sup>C-methionine should have the potential to accurately differentiate malignant tumors from benign lesions, particularly granulomatous lesions.

## ACKNOWLEDGMENTS

This study was performed through special coordination funds for promoting science and technology, provided by the Ministry of Education, Culture, Sports, Science, and Technology of the Japanese Government. This work was also supported in part by grants-in-aid for scientific research from the Japan Society for the Promotion of Science and the Japanese Ministry of Education, Culture, Sports, Science, and Technology and by a grant from the Rotary Yoneyama Memorial Foundation, Inc. The authors are grateful to the

staffs of the Department of Nuclear Medicine, Central Institute of Isotope Science; Institute for Animal Experimentation, Hokkaido University; and Faculty of Radiology, Hokkaido University Hospital for supporting this study. We also thank Eriko Suzuki for continuously supporting this study and Makoto Sato, SHI Accelerator Service Ltd., for <sup>18</sup>F-FDG synthesis.

## REFERENCES

1. Delbeke D, Rose DM, Chapman WC, et al. Optimal interpretation of FDG PET in the diagnosis, staging and management of pancreatic carcinoma. *J Nucl Med.* 1999;40:1784-1791.
2. Dimitrakopoulou-Strauss A, Strauss LG, Heichel T, et al. The role of quantitative <sup>18</sup>F-FDG PET studies for the differentiation of malignant and benign bone lesions. *J Nucl Med.* 2002;43:510-518.
3. Brudin LH, Valind S, Rhodes CG, et al. Fluorine-18 deoxyglucose uptake in sarcoidosis measured with positron emission tomography. *Eur J Nucl Med.* 1994; 21:297-305.
4. Lewis PJ, Salama A. Uptake of fluorine-18-fluorodeoxyglucose in sarcoidosis. *J Nucl Med.* 1994;35:1647-1649.
5. Ohtsuka T, Nomori H, Watanabe K, et al. False-positive findings on [<sup>18</sup>F]FDG-PET caused by non-neoplastic cellular elements after neoadjuvant chemoradiotherapy for non-small cell lung cancer. *Jpn J Clin Oncol.* 2005;35:271-273.
6. Lorenzen J, de Wit M, Buchert R, Igel B, Bohuslavizki KH. Granulation tissue: pitfall in therapy control with F-18-FDG PET after chemotherapy. *Nuklearmedizin.* 1999;38:333-336.
7. Conessa C, Hervé S, Foehrenbach H, Poncet JL. FDG-PET scan in local follow-up of irradiated head and neck squamous cell carcinomas. *Ann Otol Rhinol Laryngol.* 2004;113:628-635.

8. van Waarde A, Cobben DC, Suurmeijer AJ, et al. Selectivity of <sup>18</sup>F-FLT and <sup>18</sup>F-FDG for differentiating tumor from inflammation in a rodent model. *J Nucl Med.* 2004;45:695–700.
9. van Waarde A, Jager PL, Ishiwata K, Dierckx RA, Elsinga PH. Comparison of sigma-ligands and metabolic PET tracers for differentiating tumor from inflammation. *J Nucl Med.* 2006;47:150–154.
10. Shields AF, Grierson JR, Dohmen BM, et al. Imaging proliferation in vivo with [<sup>18</sup>F]FLT and positron emission tomography. *Nat Med.* 1998;4:1334–1336.
11. Sherley JL, Kelly TJ. Regulation of human thymidine kinase during the cell cycle. *J Biol Chem.* 1988;263:8350–8358.
12. Jacobs AH, Dittmar C, Winkeler A, Garlip G, Heiss WD. Molecular imaging of gliomas. *Mol Imaging.* 2002;1:309–335.
13. Tsuyuguchi N, Sunada I, Ohata K, et al. Evaluation of treatment effects in brain abscess with positron emission tomography: comparison of fluorine-18-fluorodeoxyglucose and carbon-11-methionine. *Ann Nucl Med.* 2003;17:47–51.
14. Kubota K, Kubota R, Yamada S, Tada M. Effects of radiotherapy on the cellular uptake of carbon-14 labeled L-methionine in tumor tissue. *Nucl Med Biol.* 1995;22:193–198.
15. Kubota R, Kubota K, Yamada S, et al. Methionine uptake by tumor tissue: a microautoradiographic comparison with FDG. *J Nucl Med.* 1995;36:484–492.
16. Reinhardt MJ, Kubota K, Yamada S, Iwata R, Yaegashi H. Assessment of cancer recurrence in residual tumors after fractionated radiotherapy: a comparison of fluorodeoxyglucose, L-methionine and thymidine. *J Nucl Med.* 1997;38:280–287.
17. Zhao S, Kuge Y, Kohanawa M, et al. Extensive FDG uptake and its modification with corticosteroid in a granuloma rat model: an experimental study for differentiating granuloma from tumors. *Eur J Med Mol Imaging.* September 1, 2007 [Epub ahead of print].
18. Zhao S, Kuge Y, Tsukamoto E, et al. Effects of insulin and glucose loading on FDG uptake in experimental malignant tumours and inflammatory lesions. *Eur J Nucl Med.* 2001;28:730–735.
19. Takei T, Kuge Y, Zhao S, et al. Enhanced apoptotic reaction correlates with suppressed tumor glucose utilization after cytotoxic chemotherapy: use of <sup>99m</sup>Tc-annexin V, <sup>18</sup>F-FDG, and histologic evaluation. *J Nucl Med.* 2005;46:794–799.
20. Yamada Y, Uchida Y, Tatsumi K, et al. Fluorine-18-fluorodeoxyglucose and carbon-11-methionine evaluation of lymphadenopathy in sarcoidosis. *J Nucl Med.* 1998;39:1160–1166.
21. Kubota K, Matsuzawa T, Fujiwara T, et al. Differential diagnosis of AH109A tumor and inflammation by radioscintigraphy with L-[methyl-<sup>11</sup>C]methionine. *Jpn J Cancer Res.* 1989;80:778–782.
22. Osman S, Danpure HJ. The use of 2-[<sup>18</sup>F]fluoro-2-deoxy-D-glucose as a potential in vitro agent for labeling human granulocytes for clinical studies by positron emission tomography. *Int J Rad Appl Instrum B.* 1992;19:183–190.
23. Borregaard N, Herlin T. Energy metabolism of human neutrophils during phagocytosis. *J Clin Invest.* 1982;70:550–557.
24. Kubota R, Yamada S, Kubota K, Tamahashi N, Ido T. Intratumoral distribution of fluorine-18-fluorodeoxyglucose in vivo: high accumulation in macrophages and granulation tissues studied by microautoradiography. *J Nucl Med.* 1992;33:1972–1980.
25. Saga T, Kawashima H, Araki N, et al. Evaluation of primary brain tumors with FLT-PET: usefulness and limitations. *Clin Nucl Med.* 2006;31:774–780.
26. Yap CS, Czernin J, Fishbein MC, et al. Evaluation of thoracic tumor with <sup>18</sup>F-fluorothymidine and <sup>18</sup>F-fluorodeoxyglucose-positron emission tomography. *Chest.* 2006;129:393–401.
27. Drent M, du Bois RM, Poletti V. Recent advances in the diagnosis and management of nonspecific interstitial pneumonia. *Curr Opin Pulm Med.* 2003;9:411–417.
28. Inoue T, Kim EE, Wong FC, et al. Comparison of fluorine-18-fluorodeoxyglucose and carbon-11-methionine PET in detection of malignant tumors. *J Nucl Med.* 1996;37:1472–1476.
29. Kubota K, Ishiwata K, Kubota R, et al. Feasibility of fluorine-18-fluorophenylalanine for tumor imaging compared with carbon-11-L-methionine. *J Nucl Med.* 1996;37:320–325.